By computing the average over one period, one has to include the large $\pi(1-\epsilon_i)s_x^i$ rotations in $H_F^{(0)}$,

$$H_{F,1P}^{(0)} = \frac{1}{t_1+\pi}\left[t_1\left(\sum_{i=1}^{L-1} J_{i,i+1}s_z^i s_z^{i+1} + \sum_{i=1}^{L} h_i s_z^i\right) + \pi\sum_{i=1}^{L}(1-\epsilon_i)s_x^i\right], \tag{4}$$

which is detrimental to the convergence of the Magnus series [47]. As stated earlier, the magnetization-flipping dynamics is period doubled with respect to the time-dependent Hamiltonian. Therefore, if averaged over two periods, one not only mostly cancels the spin rotations but also averages out any random y/z fields. The newly obtained two-period averaged effective Hamiltonian has the form of a transverse-field Ising model (TFIM),

$$H_{F,2P}^{(0)} = \frac{1}{t_1+\pi}\left(t_1\sum_{i=1}^{L-1} J_{i,i+1}s_z^i s_z^{i+1} - \pi\sum_{i=1}^{L}\epsilon_i s_x^i\right), \tag{5}$$

hereafter only referred to as $H_F^{(0)}$. Alternatively, this Hamiltonian can also be derived by applying a toggling-frame transformation and subsequently taking the average over one cycle [8]. This effective description retains the spin-flip symmetry present in the original time-dependent model.

III. RESULTS

In this section, we investigate numerically the lifetimes of various multispin and single-spin observables at stroboscopic times. We employ exact evolution according to the full Floquet unitary given in Eq. (2) in addition to the effective evolution with an TFIM as derived in Eq. (5) for comparison. Here, we study systems with $L = 14$ spins and set $J_{ij} =: J = 1$, $h_i = 0$, $\epsilon = 0.1$, $t_1 = 1$, and $\epsilon' = 10^{-5}$, if not otherwise specified.

A. Bulk lifetime enhancement for polarized initial states

We start by considering the dynamics of the global magnetization $\langle\sum_i \sigma_z^i\rangle/L$ for a polarized initial state $|\Psi_{\text{init}}\rangle = |\uparrow \ldots \uparrow\rangle$, as shown on a logarithmic time axis in Fig. 2. Only even period numbers are probed, so that the underlying spin-flipping dynamics is hidden in the shown simulation. The magnetization shows an initial decline that lasts $\approx 10^2$ periods of the drive, largely independent of the presence of a metronome spin. Subsequently, for both with and without metronome spin we observe slow oscillations of the magnetization, which manifest themselves as extended plateaus of nonvanishing magnetization due to the log-linear axes choice in Fig. 2. The macroscopic magnetization indicates that large parts of the chain retain some of its initial polarization. The duration of this plateau is strongly dependent on the angle deviation of the metronome spin drive ϵ' and, in the case of an active metronome spin, lasts $\approx 10^7$ periods instead of $\approx 10^3$ periods without the metronome. The single-spin magnetization of the metronome spin, $\langle\sigma_z^1\rangle$, as shown on the right axis of Fig. 2, qualitatively demonstrates the same behavior and has a lifetime similar to that of $\langle\sum_i \sigma_z^i\rangle/L$. For all data taken,

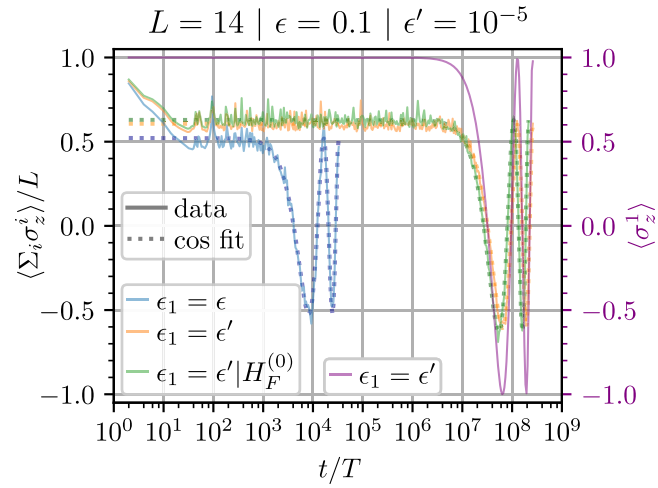

FIG. 2. The global z magnetization of the spin chain of length $L = 14$ starting in a fully polarized stated subjected to different driving schemes. We show the exact stroboscopic dynamics of the chain at even period numbers with and without a metronome spin at one boundary site and the average Hamiltonian given in Eq. (5). Configurations that include a metronome spin display a lifetime enhancement of several orders of magnitude. All data are well described through numerical cosine fits. On the second axis (in purple font) the single-spin magnetization of the metronome spin itself is displayed. The lifetime of the magnetization of the metronome coincides with the lifetime of the total magnetization. For better visibility, only the first two oscillation cycles are plotted for each curve.

the evolution under the two-period average of the Floquet Hamiltonian $H_F^{(0)}$ is in satisfactory agreement with the full Floquet evolution (the green line shows this for the case with metronome spin), indicating that it is a sufficiently good description of the full stroboscopic evolution. Therefore, we can safely focus on the simpler time-independent $H_F^{(0)}$ to better understand the observed behavior.

Our chosen polarized initial state is the superposition of the two lowest-energy eigenstates of $H_F^{(0)}$ which, for $\epsilon \ll J$, are well approximated by the two parity states, $|\pm\rangle_L = (|\uparrow \ldots \uparrow\rangle \pm |\downarrow \ldots \downarrow\rangle)/\sqrt{2}$. At finite ϵ, states with domain-wall excitations are admixed (domain-wall dressing), leading to the observed initial fast decay. The energy gap between the two lowest-lying states is $\propto \epsilon^L$ in the uniform case by a perturbative argument, considering that all L spins are being flipped through off-resonant coupling to excited states. Thus, the gap vanishes in the limit $L \to \infty$, making the two states degenerate. In the case of $L = 14$ presented here, the gap is still finite and leads to slow Rabi oscillations of period T_R between the two polarized states, which explains the observed behavior. The data show good agreement with the numerical cosine fits $\propto \cos(2\pi t/T_R)$, as also plotted in Fig. 2, with $T_R(\epsilon_1 = \epsilon) = (1.641 \pm 0.006)10^4 T$ and $T_R(\epsilon_1 = \epsilon') = (1.281 \pm 0.004)10^8 T$. This difference in the length of the period of four orders of magnitude is expected in the average Hamiltonian picture, as the energy gap given above is inversely proportional to the Rabi-oscillation period $T_R \propto \epsilon^{-L}$. By endowment of one spin with reduced ϵ', one obtains

$$T_R \propto \epsilon^{-L+1}(\epsilon')^{-1}, \tag{6}$$